JACS
JOURNAL OF THE AMERICAN CHEMICAL SOCIETY

ARTICLE

pubs.acs.org/JACS

Tuning Multiphase Amphiphilic Rods to Direct Self-Assembly

Jie-Yu Wang,[†,§] Yapei Wang,[†,§] Sergei S. Sheiko,[†] Douglas E. Betts,[†] and Joseph M. DeSimone*[,†,‡]

[†]Department of Chemistry, University of North Carolina at Chapel Hill, Chapel Hill, North Carolina 27599, United States

[‡]Department of Chemical and Biomolecular Engineering, North Carolina State University, Raleigh, North Carolina 27695, United States

Supporting Information

ABSTRACT: New methods to direct the self-assembly of particles are highly sought after for multiple applications, including photonics, electronics, and drug delivery. Most techniques, however, are limited to chemical patterning on spherical particles, limiting the range of possible structures. We developed a lithographic technique for fabrication of chemically anisotropic rod-like particles in which we can specify both the size and shape of particles and implement multiple diverse materials to control interfacial interactions. Multiphase rod-like particles, including amphiphilic diblock, triblock, and multiblock were fabricated in the same template mold having a tunable hydrophilic/hydrophobic ratio. Self-assembly of diblock or triblock rods at a water/oil interface led to the formation of bilayer or ribbon-like structures.

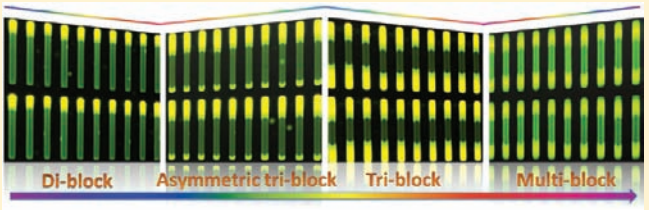

INTRODUCTION

Directing the self-assembly of anisotropic particles has attracted attention for applications in nano/microdevices, including electronics,[1] sensing and imaging,[2] and optics[3] and for use in drug delivery.[4] Self-assembly processes are strongly dependent on both interparticle interactions and particle dimensions (size and shape).[5] Studies using Janus spheres have shown the combination of two chemical components on the particle's surface favors directed assembly both in solution and at an oil/water interface.[6] Additionally, increasing efforts have been devoted to fabricating nonspherical multiphase particles, opening the possibility of directing the self-assembly combined with multifunctionality for intended applications.[7]

Metal and semiconductor nanocrystals have been formulated to produce anisotropic block particles successfully,[8] yet organic counterparts with low polydispersity and tunable components generated from soft materials are still challenging. New "top-down" fabrication strategies allow the generation of multiphase organic particles via introducing patchiness on specific sites of the particles,[9] microfluidics,[10] photolithography,[11] micromolding,[12] or microemulsions.[13] However, challenges in controlling the particle geometry, tuning of the particle compositions, and scaling up the particle fabrication as well as the high cost and time-consuming process limit their wide use in future applications. Recently, we have demonstrated a scalable off-shoot of a soft imprint lithography technique referred to as particle replication in nonwetting templates (PRINT) to fabricate monodisperse particles with precise and independent control over the particle size, shape, and composition, which has shown great potential for applications in drug delivery and electronics.[14] PRINT is uniquely able to fabricate particles in large quantity from a diversity of organic materials while incorporating properties essential to the intended application, e.g., bioactivity, modulus, and surface functionalization.[15]

Herein, we present a novel strategy using PRINT to synthesize anisotropic amphiphilic rods from organic materials with tunable multiphases, such as diblock, triblock, and multiblock structures. By using diblock or triblock particles at an oil/water interface, we were able to direct self-assembly of particles to form either bilayer or ribbon-like structures.

EXPERIMENTAL METHODS

Materials. Fluorescein *o*-acrylate (Aldrich), methacryloxyethyl thiocarbamoyl rhodamine B (PolyFluor 570, Polysciences), 1-hydroxycyclohexyl phenyl ketone (HCPK, Aldrich), poly(ethylene glycol) diacrylate (M_n = 700 g/mol, $PEG_{700}DA$, Aldrich), trimethylolpropane ethoxylate triacrylate (M_n = 428 g/mol, TETA, Aldrich), methacryloylchloride (Aldrich), tetraethylene glycol (Aldrich), perfluorodecalin (PFD, Aldrich), gelatin (type A from porcine skin, Aldrich), and dimethyl formamide (DMF, Aldrich) were used as received. Monohydroxytetraethyleneglycol methacrylate (HP_4MA) was synthesized according to the literature method.[16] Photocurable perfluoropolyether (PFPE) resin was synthesized as previously reported.[17] PFPE mold with 20 × 20 × 240 μm features was provided by Liquidia Technologies Inc. (see Table 1 and Figure S2, Supporting Information).

Characterization Methods. Scanning electron microscopy (SEM) images were recorded on a Hitachi model S-4700. Fluorescence and optical microscopy images were captured on a Zeiss Axioskop 2 MAT incident light microscope fitted with an AxioCam MR digital camera.

Particle Tracking at the Interface. A gel trapping method was utilized to track the particles at the water/oil interface.[18] Typically, a well containing PFD and water with PRINT particles at the oil/water interface was placed in a refrigerator at 3 °C. Hot gelatin solution (100 mg/mL) was added dropwise to the water phase. The bottom PFD phase was

Received: July 15, 2011
Published: October 11, 2011

dx.doi.org/10.1021/ja2066187 | J. Am. Chem. Soc. 2012, 134, 5801–5806

Table 1. Composition of Block Particles

	composition	wt %
hydrophilic part	HP_4MA	78.8
	$PEG_{700}DA$	20
	HCPK	1
	PolyFluor 570	0.2
	DMF	varied according to different concentrations
hydrophobic part	TETA	98
	HCPK	1
	fluorescein *o*-acrylate	1

removed after the water phase was completely gelled. PFPE having 0.2 wt % HCPK was poured on the gelatin which was subjected to UV irradiation (λ = 365 nm, power ≈ 2 J/cm^2) under N_2 purge for 5 min. The resulting cured PFPE film was approximately regarded as the "frozen PFD phase", thus indirectly exhibiting the interfacial distortion by the particles.

Particle Fabrication. *Triblock Particles.* A small aliquot of a DMF solution of hydrophilic monomer mixture was dropped onto a piece of mold and filled using a poly(ethylene terephthalate) (PET) cover sheet and a single-roll laminator. The PET cover sheet wicked away any excess monomer solution yielding a filled mold without any scum or flash layer. After heating at 70 °C for 30 min, the DMF was completely evaporated from the mold, and the remaining hydrophilic monomer was partially cured by UV irradiation for 1 min (λ = 365 nm, power ≈ 2 J/cm^2) under a nitrogen atmosphere. The remaining mold cavities were then filled with the hydrophobic monomer mixture via the same procedure, followed by complete curing of all monomers by intense UV irradiation for 4 min (λ = 365 nm, power ≈ 20 J/cm^2). The particles were harvested by laminating the cured mold over 100 μL of cyanoacrylate (ZAP superglue PT-08) placed on a glass slide. The cyanoacrylate was allowed to set for 3−5 min, after which the mold was peeled away leaving the particles embedded in the cured cyanoacrylate harvesting layer. The (extracted, obtained, harvested) particles were purified by dissolving the cyanoacrylate in acetone followed by repeated centrifugation and acetone washing steps.

Diblock Particles. The diblock particle mold filling operation is the same as that for the triblock particles. After filling the mold and evaporation of the DMF solvent, the mold was fixed to a centrifuge (Eppendorf, centrifuge 5417R) with the distance of 5 cm to the rotation center and spun at various angular velocities for 5−20 min before partially curing by UV irradiation for 1 min under an atmosphere of nitrogen. After filling the remaining mold cavities with the second hydrophobic monomer mixture, all the monomers were UV cured, as described above. The resulting diblock particles were harvested in the same fashion as the triblock particles described previously.

RESULTS AND DISCUSSION

The fabrication of multiphase amphiphlic PRINT particles begins with a patterned PFPE mold with feature sizes of 20 × 20 × 240 μm. These robust molds have been shown to have remarkably low adhesion with respect to other materials, high gas permeability, and high solvent resistance, ensuring successful mold-filling and particle harvesting operation.[19] A mixture of HP_4MA with 20 wt % cross-linker, poly(ethylene glycol) diacrylate, was used as the hydrophilic block, while hydrophobic part was composed of TETA.

As shown in Figure 1, the fabrication process consists of several steps. First, a dilute solution of hydrophilic monomer in

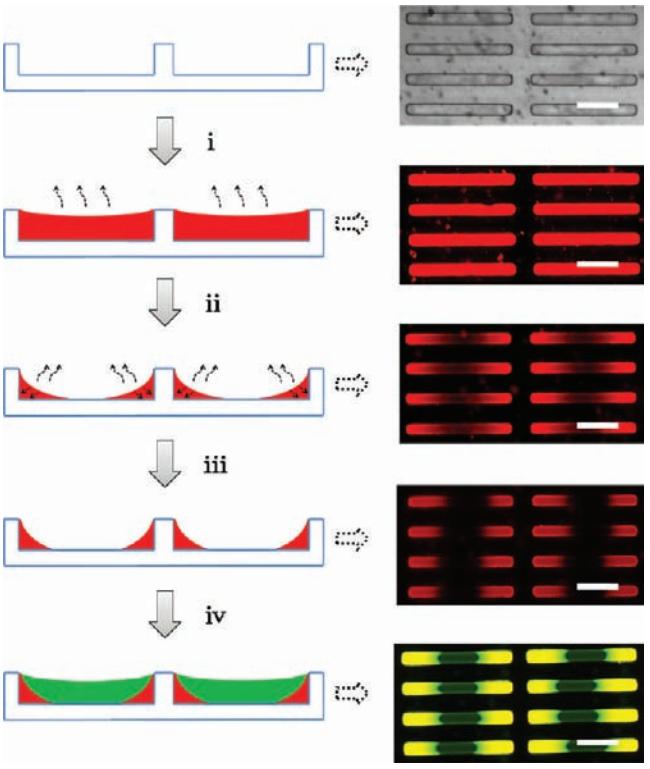

Figure 1. Schematic illustration of the formation of triblock rods and the corresponding microscopic images of the molds in each step (all scale bars: 100 μm). To distinguish the middle filled hydrophobic blocks from the hydrophilic blocks, photocurable red and green dyes were premixed into the hydrophilic and hydrophobic monomers prior to photocuring, respectively.

DMF was used to fully fill the PFPE mold. Second, the solvent was evaporated, and the remaining monomer was drawn by capillary forces to both ends of the rectangular cavity. Third, the mold was exposed to a low intensity UV light source to convert the monomer into a soft gel, thus allowing the second hydrophobic monomer mixture to be added to fill the empty section in the middle of each mold cavity without removal of the first block or mixing of the phases. Fourth, the final monomer composition was fully cured by intense UV irradiation resulting in a triblock architecture with the blocks covalently connected together. Finally, the array of triblock particles was transferred from the mold cavities onto a harvesting film coated with a sacrificial adhesive, and free particles were obtained by the dissolution of the sacrificial adhesive from the particles. Importantly, the hydrophilic/hydrophobic ratio in triblock structure could be precisely tuned by simply changing the concentration of the original monomer solution. As shown in Figure 2C−F, the hydrophilic heads of ABA amphiphilic triblock rods can be controlled by varying the concentration of the first monomer mixture. In order to compare self-assembly behaviors of particles, solely hydrophobic and hydrophilic (Figure 2A and B, respectively) particles were fabricated as reference samples.

The principle of fabricating triblock rods has been extended to the generation of multiblock ABABA rods. In this technique, the mold is partially filled, as before, by a first diluted hydrophobic monomer solution containing a green dye. A second block is generated by a diluted hydrophilic monomer solution containing red dye (Figure 3A) while remaining an open space in the middle

dx.doi.org/10.1021/ja2066187 |*J. Am. Chem. Soc.* 2012, 134, 5801–5806

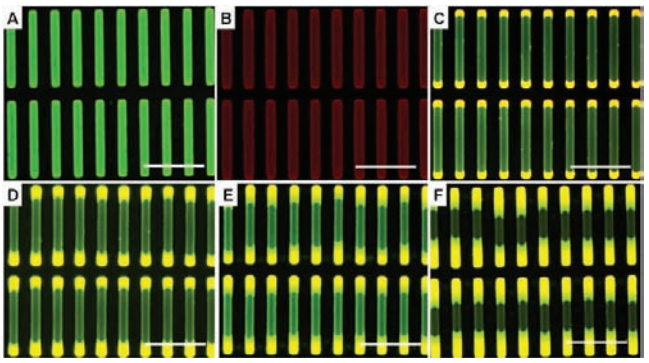

Figure 2. Array of 20 × 20 × 240 μm rod particles on harvesting film with tunable dimensions in ABA triblock structures. (A) One component hydrophobic particles. (B) One component hydrophilic particles. (C−F) ABA triblock particles with different hydrophilic/hydrophobic/hydrophilic ratios corresponding to the four HP_4MA concentrations of (C): 10, (D): 20, (E): 30, and (F): 50 wt %. (C−F) were captured by overlaying the images under red and green channels. Scale bar: 200 μm.

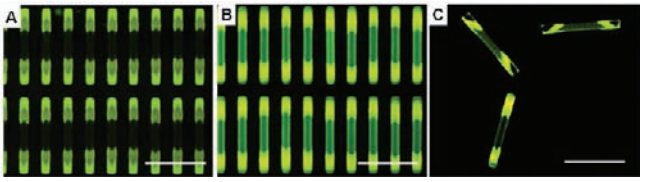

Figure 3. Array of anisotropic rods having multiphases. (A) Diblocks transferred from partially filled mold in two ends onto a cynoacrylate film. (B) Multiphase particles harvested on a cynoacrylate film. (C) Free multiphase particles separated from cynoacrylate film. The images were captured by overlaying the images under red and green channels. Scale bar: 200 μm.

of mold cavity, which is able to be filled by a third hydrophobic monomer (undiluted) containing green dye. As shown in Figure 3B and C, five blocks arranged ABABA were observed to coexist in a particle, demonstrating this is a powerful tool to build a library of anisotropic rods having tunable multiphases consisting of different materials.

The above examples are limited to symmetric block distributions. To break the symmetry, a partially filled mold containing two hydrophilic end blocks was subjected to rotation around an axis perpendicular to the mold plane. As shown in Figure 4, the resulting centrifugal force drew the first monomer composition to the outer end of the mold cavity, leaving the rest of the cavity open. The open space was subsequently filled with a second hydrophobic monomer, yielding a range of solidified amphiphilic diblock rods via complete photocuring, as shown in Figure 5B−D. The length of the residual hydrophilic blocks after rotation was observed to decrease with increasing rotational velocity (Figure 5E). As such, this developed technique could provide us with a strategy for constructing asymmetric particles with various hydrophilic/hydrophobic ratios. Additional rotation comparison between 30 and 80 wt % (Figure 5E) demonstrates that the residual monomer length in the mold cavity is independent of concentration and solely determined by the angular velocity. Moreover, the length of the hydrophilic block remained unchanged as the rotation time was increased at a given angular velocity (Figure S5, Supporting Information).

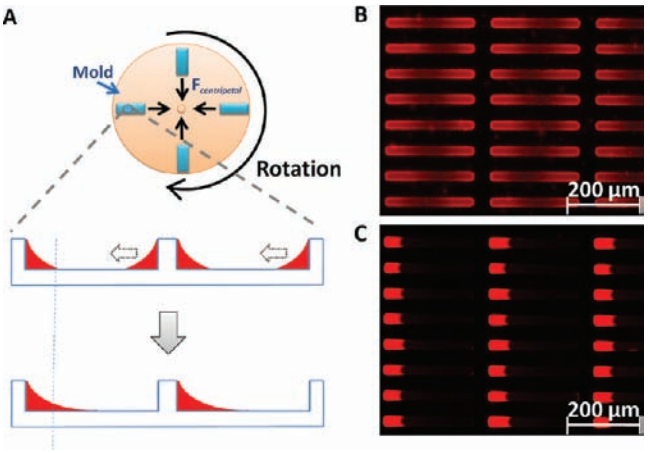

Figure 4. (A) Schematic illustration of the cross-section of the mold before and after rotation. Partially filled molds with HP_4MA monomer containing red dye dissolved in DMF solution at concentrations of 80 wt % before (B) and after rotation (C) at 14 000 rpm. The solvent was completely removed on a hot plate at 70 °C for 30 min before rotation.

To analyze the driving forces that enable the length control, we considered a capillary with an $a \times a$ square cross-section and an one open side. The capillary rotates along an axis perpendicular to its length with an angular velocity ω. As shown in Figure 5A, the length L of the "capillary rise" (length of the liquid confined within the capillary) is determined by the balance of the capillary and centrifugal forces as

$$f = f_{cap} - f_{cent} = \gamma a(3\cos\theta - 1) - m\omega^2 r \quad (1)$$

where θ is the equilibrium contact angle between the monomer and the surface of PFPE mold, γ = 40 mN/m is the surface energy of the monomer, $m = \rho V = \rho L a^2$ is the mass of the liquid in a rotating capillary, a = 20 μm is the capillary lateral size, ρ = 1.1 g/cm^3 is the mass density of the monomer, and r = 0.05 m is the rotation radius. At equilibrium (f = 0), the length of the residing monomer is given by

$$L = \frac{\gamma(3\cos\theta - 1)}{\rho a \omega^2 r} \quad (2)$$

This equation shows that the length decreases with the angular velocity as $L \sim \omega^{-2}$, which is consistent with the data points in Figure 5E.

eq 2 is acceptable for long capillaries ($L \gg a$), in which one can neglect shape variations that are commensurable with the capillary cross-section. For systems with a small amount of a confined liquid ($L \sim a$), eq 2 needs to be modified to include two additional ω-independent contributions to the measured block length. First, there is a small volume of liquid which remains trapped in the corner of the capillary, leading to an ill-defined increment of the rod length. Second, one should consider transformation of the liquid shape at the free end of the confined monomer after the rotation stops, which leads to an apparent extension of the rod. The equilibrium shape is determined by the minimum of the interfacial free energy at constant volume. The exact shape is complex due to convolution of two orthogonal meniscuses. However, for our purpose, it is sufficient to approximate the free end of the confine liquid with a trapezoidal shape (Figure 5A). Since these two contributions do not depend on the

dx.doi.org/10.1021/ja2066187 |J. Am. Chem. Soc. 2012, 134, 5801–5806

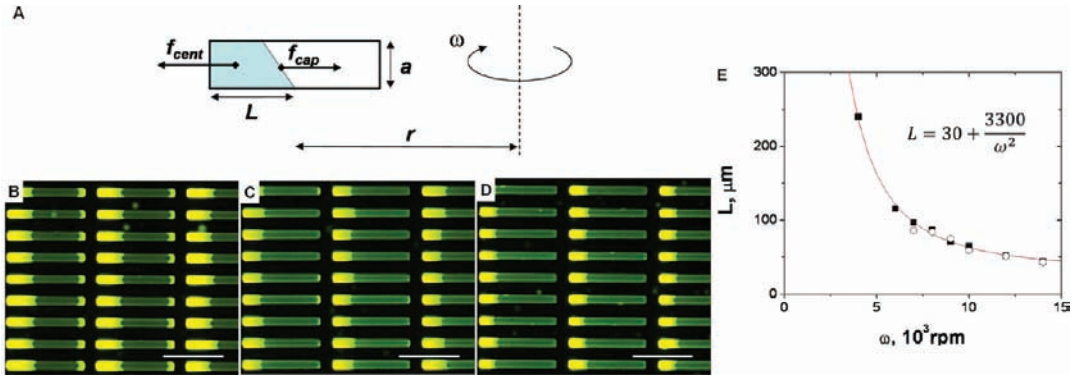

Figure 5. (A) Schematic illustration of the parameters during the rotation process. (B−D) Generated amphiphilic diblock particles harvested on a harvesting film of cyanoacrylate, which were fabricated by filling the mold with 80 wt % of hydrophilic monomer solution and then rotating at various angular velocities (B) 8000 rpm; (C) 10 000 rpm; (D) 14 000 rpm before being filled with a second hydrophobic monomer and cured. (E) Experimental (circle: 30 wt %; filled square: 80 wt %) and theoretical (red curve) length of the liquid confined within a square ($a \times a$) capillary decreases with angular rotation speed ω. The trapezoidal shape of the liquid free end is determined by the minimum of interfacial energy. eq 3 was used to fit the experimental data with two fitting parameters $\cos\theta = 0.34 \pm 0.01$ and $L_0 = 30\ \mu$m for the following properties of the studied systems. (B−D) were captured by overlaying the images under red and green channels. Scale bar of (B−D): 200 μm.

rotation speed, we rewrite eq 2 as

$$L = \frac{(3\cos\theta - 1)\gamma}{\rho a \omega^2 r} + L_0 \qquad (3)$$

where L_0 includes the amount of the permanently residing liquid and the length variation due to spreading at the free end. eq 3 was used to fit the data using two fitting parameters $\cos\theta = 0.34 \pm 0.01$ and $L_0 = 30\ \mu$m. Since these two parameters are functionally decoupled ($\cos\theta$ determines the shape of the curve, and $L = L_0$ corresponds to the plateau at $\omega \rightarrow \infty$), the fit is fairly accurate. Furthermore, the determined $\cos\theta = 0.34 \pm 0.01$ shows an excellent agreement with an equilibrium contact angle of $\theta = 72 \pm 2°$ ($\cos\theta = 0.31 \pm 0.03$), which was independently measured for a monomer drop on a surface of a flat PFPE substrate.

Once the amphiphilic anisotropic block rods were created, their directed self-assembly was explored at a water/perfluorodecalin (PFD) interface to demonstrate the dependence of the self-assembly behavior on the particle architecture.[20] The self-assembly of micrometer-size particles at a water/oil interface is attributed to the lateral capillary forces acting between the particles due to deformation of the oil/water interface.[21] Note that the gravitational forces are negligibly small for microscopic particles with dimensions of the order of 100 μm.[22] The surface wetting of particles and hence the shape of the meniscus is conventionally thought to be controlled by the chemical compositions of the fluid and the particles and the geometry of the particles.[23] In our work, the resulting PRINT particles all have an approximately rectangular shape, while their surface chemistry and anisotropic architecture can be tuned, thus providing a platform for directing particle assembly at an interface. As controls, the single-phase hydrophilic particles were shown to aggregate side-to-side into bundles (Figure 6A). Morphology of the assembled particles at the interface was studied using a gel trapping method which enabled replication of the oil/water interface on a cured PFPE film. The hydrophilic particles were found contacting the oil phase by one of the rectangular faces, while the other three rectangular faces seem to have an affinity to the water phase. In this case, the particles could not be trapped in the oil phase as they are mostly wrapped by the gel phase. As shown in Figure 6C, the interfacial distortion indicative of a

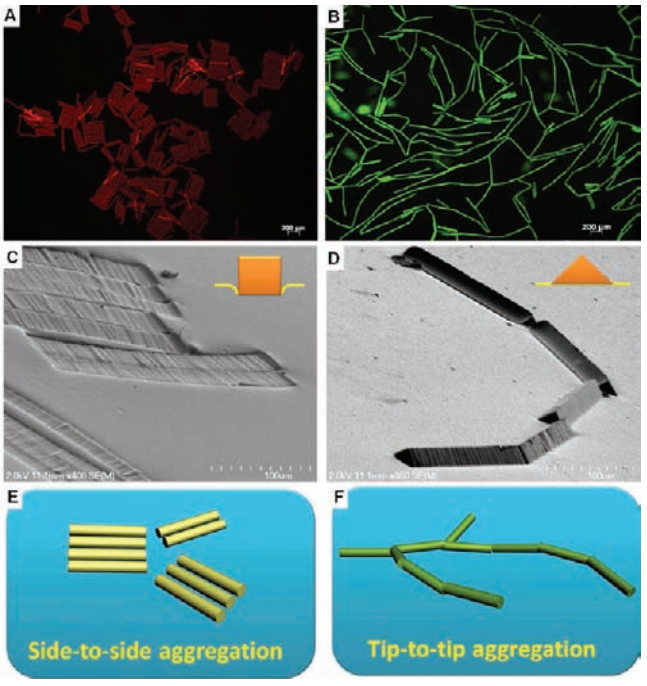

Figure 6. Fluorescence microscopic images of different particles assembled at the water/PFD interface for the (A) hydrophilic particles and the (B) hydrophobic particles. Orbital rotation for approximately 12 h was used to break up any unstable aggregates to allow the particles to approach steady state at the water/PFD interface. Scanning electron micrographs are shown for the (C) PFPE mold obtained for the particle trapping experiment for the single-phase hydrophilic particles on the oil surface and for the (D) PFPE mold for the single-phase hydrophobic particles trapped at the oil phase. Self-assembly models are illustrated for the (E) hydrophilic particles and the (F) hydrophobic particles at the water/oil interface.

negative meniscus on the oil surface was replicated. As a result, the hydrophilic particles tend to interact over more of their perimeter in a side-to-side fashion leading to a more pronounced reduction of the total energy at the interface. However, the hydrophobic particles adopted a tip-to-tip aggregation at the

dx.doi.org/10.1021/ja2066187 |J. Am. Chem. Soc. 2012, 134, 5801–5806

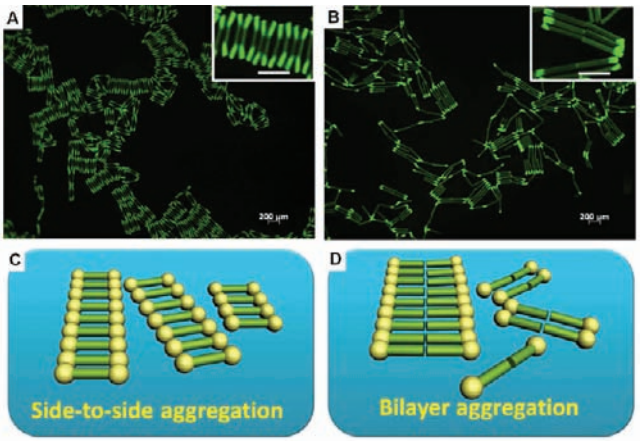

Figure 7. Fluorescence microscopic images of different particles assembled at the water/PFD interface. (A) ABA hydrophilic/hydrophobic/hydrophilic triblock particles produced using a 50 wt % HP_4MA solution as shown in Figure 2F. (B) AB diblock particles fabricated using an 80 wt % HP_4MA solution and rotated at 14 000 rpm as shown in Figure 5D. The scale bar of the inserts: 200 μm. Self-assembly models are illustrated for the particles at a water/oil interface for the (C) triblock and (D) diblock particles.

water/PFD interface forming a branched network (Figure 6B). Unlike the hydrophilic particles, hydrophobic particles prefer wetting by the oil. As shown in Figure 6D, the hydrophobic particles contact the oil phase by a rectangular long edge corner with nearly half of the perimeter embedded in oil phase. Due to this particular surface wetting, the long sides of the particles have less excess area[22] than the ends, thus the capillary attraction resulting from the elimination of excess area is stronger at the particle tips. As a result of the relatively weak attraction between the long sides, conventional steering breaks the metastable side-to-side aggregates, allowing the formation of branched structures with minimum energy in a tip-to-tip manner.

The self-assembly of amphiphilic triblock and diblock particles was also investigated at the water/PFD interface. The triblock particles, behaving like bolaamphiphiles, preferred a side-to-side assembly, forming ordered ribbon structures at the interface, as shown in Figure 7A. In regard to the particle orientation at the interface, as shown in Figure S6A and S6B, Supporting Information, a very similar lateral capillary force to single-phase hydrophilic particles is assumed to provide a driving force in this directed self-assembly process. However, the triblock architecture allows each particle to match the others in a better side-to-side fashion than does the single-phase hydrophilic particle. It is the different interfacial distortion around the hydrophilic and hydrophobic parts that limits each block of the triblock particles to direct the assembly only with others having same components. It should be noted that the particles adopted a bent conformation at the interface, which is presumably caused by the curved interface between the hydrophilic and hydrophobic blocks and the swelling of the hydrophilic blocks in water. Interestingly, the diblock particle, having an asymmetric structure similar to a molecular surfactant, self-assembled into a 2D bilayer structure at the water/PFD interface (Figure 7B). In a bilayer structure, the side-to-side lateral interactions pull the particles together forming bundles, while the heads of the hydrophobic blocks tended to aggregate by a tip-to-tip lateral interaction. The cooperation of both assembly fashions thus induces the formation of a bilayer structure, being like the shell structure of vesicles assembled by traditional surfactants.

SUMMARY

We demonstrated a novel strategy to generate a range of monodisperse amphiphilic rod-like particles with tunable dimensions and chemical composition of the blocks. A combination of hydrophilic and hydrophobic materials created amphiphilic diblock, triblock, and multiblock rods in which the hydrophilic/hydrophobic ratio was able to be precisely tuned. Directed self-assembly of these anisotropic amphiphilic block particles at the water/oil interface illuminates the relationship between particle architecture and self-assembly behavior. The amphiphilic triblock rods self-assembled into ribbons, while amphiphilic diblock rods formed a bilayer structure. This new family of anisotropic block rods provides a platform for theoretical as well as experimental understanding of self-assembly behavior of anisotropic nonspherical particles. The concept of multiphases coexisting in a particle is anticipated to open an avenue to design new drug carriers, allowing the encapsulation of several drugs with hydrophilic or hydrophobic properties in one carrier. In addition, the creation of block features paves the way for fabricating microelectronics, e.g., P−N junctions, by using semiconductor materials. The scalability of symmetric tri- or multiblock particles via the roll-to-roll process is a significant departure from our standard PRINT process and would require significant changes in order to be scalable. Currently, we are developing other strategies for preparing anisotropic block particles that may also be scalable in a continuous roll-to-roll process.

ASSOCIATED CONTENT

Supporting Information. Materials used for fabricating the particles; SEM and microscopic images of the empty mold; fluorescence microscopic images of partially filled mold; SEM images of particle heads and whole triblock particles; lengths of the remaining monomer in the mold cavity under different rotation time at an angular velocity of 8000 rpm; and illustration of particle assembly at interface. These materials are available free of charge via the Internet at http://pubs.acs.org.

AUTHOR INFORMATION

Corresponding Author
desimone@unc.edu

Author Contributions
§These authors contributed equally.

ACKNOWLEDGMENT

The authors thank the National Science Foundation under grant no. DMR-0923604 and DMR 0906985 for their support of this research as well as the STC program of the National Science Foundation for shared facilities.

REFERENCES

(1) (a) Park, S.; Chung, S.-W.; Mirkin, C. A. *J. Am. Chem. Soc.* **2004**, *126*, 11772–11773. (b) Huynh, W. U.; Dittmer, J. J.; Alivisatos, A. P. *Science* **2002**, *295*, 2425–2427.

(2) (a) Sudeep, P. K.; Joseph, S. T. S.; Thomas, K. G. *J. Am. Chem. Soc.* **2005**, *127*, 6516–6517. (b) Huang, X.; El-Sayed, I. H.; Qian, W.; El-Sayed, M. A. *J. Am. Chem. Soc.* **2006**, *128*, 2115–2120.

(3) (a) Xia, Y.; Yang, P.; Sun, Y.; Wu, Y.; Mayers, B.; Gates, B.; Yin, Y.; Kim, F.; Yan, H. *Adv. Mater.* **2003**, *15*, 353–389. (b) Murphy, C. J.; Sau, T. K.; Gole, A. M.; Orendorff, C. J.; Gao, J.; Gou, L.; Hunyadi, S. E.; Li, T. *J. Phys. Chem. B.* **2005**, *109*, 13857–13870.

(4) (a) Salem, A. K.; Searson, P. C.; Leong, K. W. *Nat. Mater.* **2003**, *2*, 668–671. (b) Gorelikov, I.; Field, L. M.; Kumacheva, E. *J. Am. Chem. Soc.* **2004**, *126*, 15938–15939.

(5) (a) Lin, Y.; Skaff, H.; Emrick, T.; Dinsmore, A. D.; Russell, T. P. *Science* **2003**, *299*, 226–229. (b) Leunissen, M. E.; Blaaderen, A.; Hollingsworth, A. D.; Sullivan, M. T.; Chaikin, P. M. *Proc. Natl. Acad. Sci. U.S.A.* **2007**, *104*, 2585–2590. (c) Kim, H. S.; Lee, C. H.; Sudeep, P. K.; Emrick, T.; Crosby, A. J. *Adv. Mater.* **2010**, *22*, 4600–4604. (d) Maye, M. M.; Kumara, M. T.; Nykypanchuk, D.; Sherman, W. B.; Gang, O. *Nat. Nanotechnol.* **2010**, *5*, 116–120.

(6) (a) Walther, A.; Müller, A. H. E. *Soft Matter* **2008**, *4*, 663–668. (b) Chen, Q.; Whitmer, J. K.; Jiang, S.; Bae, S. C.; Luijten, E.; Granick, S. *Science* **2011**, *331*, 199–202. (c) Chen, Q.; Bae, S. C.; Granick, S. *Nature* **2011**, *469*, 381–385. (d) Chen, Q.; Diesel, E.; Whitmer, J. K.; Bae, S. C.; Luijten, E.; Granick, S. *J. Am. Chem. Soc.* **2011**, *133*, 7725–7727. (e) Glaser, N.; Adams, D. J.; Böker, A.; Krausch, G. *Langmuir* **2006**, *22*, 5227–5229.

(7) (a) Park, S.; Chung, S.-W.; Mirkin, C. A. *J. Am. Chem. Soc.* **2004**, *126*, 11772–11773. (b) Liu, K.; Nie, Z.; Zhao, N.; Li, W.; Rubinstein, M.; Kumacheva, E. *Science* **2010**, *329*, 197–200. (c) Kim, J.-W.; Larsen, R. J.; Weitz, D. A. *J. Am. Chem. Soc.* **2006**, *128*, 14374–14377.

(8) (a) Park, S.; Lim, J.-H.; Chung, S.-W.; Mirkin, C. A. *Science* **2004**, *303*, 348–351. (b) Nie, Z.; Fava, D.; Kumacheva, E.; Zou, S.; Walker, G. C.; Rubinstein, M. *Nat. Mater.* **2007**, *6*, 609–614. (c) Srivastava, S.; Santos, A.; Critchley, K.; Kim, K.-S.; Podsiadlo, P.; Sun, K.; Lee, J.; Xu, C.; Lilly, G. D.; Glotzer, S. C.; Kotov, N. A. *Science* **2010**, *327*, 1355–1359. (d) Glotzer, S. C.; Solomon, M. J. *Nat. Mater.* **2007**, *6*, 557–562.

(9) (a) Hong, L.; Jiang, S.; Granick, S. *Langmuir* **2006**, *22*, 9495–9499. (b) Zhang, Z.; Pfleiderer, P.; Schofield, A. B.; Clasen, C.; Vermant, J. *J. Am. Chem. Soc.* **2011**, *133*, 392–395.

(10) (a) Dendukuri, D.; Hatton, T. A.; Doyle, P. S. *Langmuir* **2007**, *23*, 4669–4674. (b) Seiffert, S.; Romanowsky, M. B.; Weitz, D. A. *Langmuir* **2010**, *26*, 14842–14847.

(11) Brown, A. B. D.; Smith, C. G.; Rennie, A. R. *Phys. Rev. E* **2000**, *62*, 951–960.

(12) Choi, C.-H.; Lee, J.; Yoon, K.; Tripathi, A.; Stone, H. A.; Weitz, D. A.; Lee, C.-S. *Angew. Chem., Int. Ed.* **2010**, *49*, 7748–7752.

(13) (a) Tanaka, T.; Okayama, M.; Kitayama, Y.; Kagawa, Y.; Okubo, M. *Langmuir* **2010**, *26*, 7843–7847. (b) Tanaka, T.; Okayama, M.; Minami, H.; Okubo, M. *Langmuir* **2010**, *26*, 11732–11736.

(14) (a) Gratton, S. E. A.; William, S. S.; Napier, M. E.; Pohlhaus, P. D.; Zhou, Z.; Wiles, K. B.; Maynor, B. W.; Shen, C.; Olafsen, T.; Samulski, E. T.; DeSimone, J. M. *Acc. Chem. Res.* **2008**, *41*, 1685–1695. (b) Wang, Y.; Merkel, T. J.; Chen, K.; Fromen, C. A.; Betts, D. E.; DeSimone, J. M. *Langmiur* **2011**, *27*, 524–528.

(15) (a) Parrott, M. C.; Luft, J. C.; Byrne, J. D.; Fain, J. H.; Napier, M. E.; DeSimone, J. M. *J. Am. Chem. Soc.* **2010**, *132*, 17928–17932. (b) Merkel, T. J.; Jones, S. W.; Herlihy, K. P.; Kersey, F. R.; Shields, A. R.; Napier, M. E.; Luft, J. C.; Wu, H.; Zamboni, W. C.; Wang, A. Z.; Bear, J. E.; DeSimone, J. M. *Proc. Natl. Acad. Sci. U.S.A.* **2011**, *108*, 586–591. (c) Zhang, H.; Nunes, J. K.; Gratton, S. E. A.; Herlihy, K. P.; Pohlhaus, P. D.; DeSimone, J. M. *New J. Phys.* **2009**, *11*, 075018.

(16) Percec, V.; Schlueter, D.; Kwon, Y. K.; Blackwell, J.; Moeller, M.; Slangen, P. J. *Macromolecules* **1995**, *28*, 8807–8818.

(17) Wang, Y. P.; Betts, D. E.; Finlay, J. A.; Brewer, L.; Callow, M. E.; Callow, J. A.; Wendt, D. E.; DeSimone, J. M. *Macromolecules* **2011**, *44*, 878–885.

(18) Bowden, N.; Arias, F.; Deng, T.; Whitesides, G. M. *Langmuir* **2001**, *17*, 1757–1765.

(19) Rolland, J. P.; Hagberg, E. C.; Denison, G. M.; Carter, K. R.; DeSimone, J. M. *Angew. Chem., Int. Ed.* **2004**, *43*, 5796–5799.

(20) (a) Bowden, N.; Terfort, A.; Carbeck, J.; Whitesides, G. M. *Science* **1997**, *276*, 233–235. (b) Bowden, N.; Choi, I. S.; Grzybowski, B. A.; Whitesides, G. M. *J. Am. Chem. Soc.* **1999**, *121*, 5373–5391.

(21) (a) Kralchevsky, P. A.; Nagayama, K. *Adv. Colloid Interface Sci.* **2000**, *85*, 145–192. (b) Butt, H.-J.; Kappl, M. *Adv. Colloid Interface Sci.* **2009**, *146*, 48–60. (c) Böker, A.; He, J.; Emrick, T.; Russell, T. P. *Soft Mater.* **2007**, *3*, 1231–1248.

(22) Lewandowski, E. P.; Bernate, J. A.; Tseng, A.; Searson, P. C.; Stebe, K. J. *Soft Matter* **2009**, *5*, 886–890.

(23) (a) Loudet, J. C.; Alsayed, A. M.; Zhang, J.; Yodh, A. G. *Phys. Rev. Lett.* **2005**, *94*, 018301. (b) Loudet, J. C.; Yodh, A. G.; Pouligny, B. *Phys. Rev. Lett.* **2006**, *97*, 018304. (c) Lewandowski, E. P.; Bernate, J. A.; Searson, P. C.; Stebe, K. J. *Langmuir* **2008**, *24*, 9302–9307. (d) Grzybowski, B. A.; Bowden, N.; Arias, F.; Yang, H.; Whitesides, G. M. *J. Phys. Chem. B* **2001**, *105*, 404–412.